# Mathematical Model of Combustion Synthesis

**Tomohiro Akiyama, Hiromichi Isogai, and Jun-ichiro Yagi**
Institute For Advanced Materials Processing, Tohoku University, Sendai, Japan 980-77

*Mathematical modeling of the combustion synthesis was studied theoretically and experimentally by taking $Mg_2Ni$ synthesis as an example. An unsteady two-dimensional mathematical model was constructed by reflecting drastic changes in thermo-physical properties from starting material of magnesium nickel mixture to a product of intermetallic compound and measured solid-phase reaction rate with/without melting. For validating the model experimentally, an end of the cylindrical sample of compressive powders was heated, and local temperatures of the sample were monitored. The comparison between calculated and measured temperatures showed plausible agreement when the model took partial melting effect of a eutectoid phase into the fundamental equations.*

## Introduction

An experimentally-validated mathematical model of the combustion synthesis has never been reported until now in spite of its importance. This was probably caused by a lack of thermophysical property and reaction rate equation. Thus, even if a model of the combustion synthesis was developed, it was difficult to validate it experimentally. For this reason, most of the mathematical models reported (Advani et al., 1992; Kuwabara et al., 1995; Puszynski et al., 1987; Varma et al., 1990) were directed to an elucidation of process *character* rather than process *simulation*. They greatly contributed to the fundamental understanding of the combustion synthesis. However, now that some processes of the combustion synthesis have been industrialized, sophistication of the model is needed for practical use. In addition, recently some researchers reported thermophysical property and reaction rate during the combustion synthesis.

The objective of this study is, therefore, to develop a mathematical model of the combustion synthesis through experiments of $Mg_2Ni$ synthesis. It is because $Mg_2Ni$ is one of the most typical hydrogen storage alloys and there are plans for the practical use of the combustion synthesis of this alloy in the near future (Akiyama et al., 1995a,b, 1996a,b, 1997a).

## Experimental Studies

Samples were prepared from commercially available reagents of magnesium ($-177$ micron) and nickel (2 to 3 micron). They were well mixed with a 2:1 molar ratio in a liquid acetone by using an ultrasonic homogenizer, dried and then compressed to cylindrical shape (10 mm $\phi$), by a single acting press at 1.0 GPa. Figure 1 shows the experimental apparatus used. A bottom end of the sample is uniformly heated by electrical resistance Nichrome heater through thin mica plate with 0.1 mm thickness. The mica plate was inserted in order to avoid electrical conduction between the heater and the sample. The resulting heat propagation within the sample from bottom to top was monitored by two thermocouples inserted at different heights on a central axis, as shown in Figure 2. The heater surface except the sample-contacting round

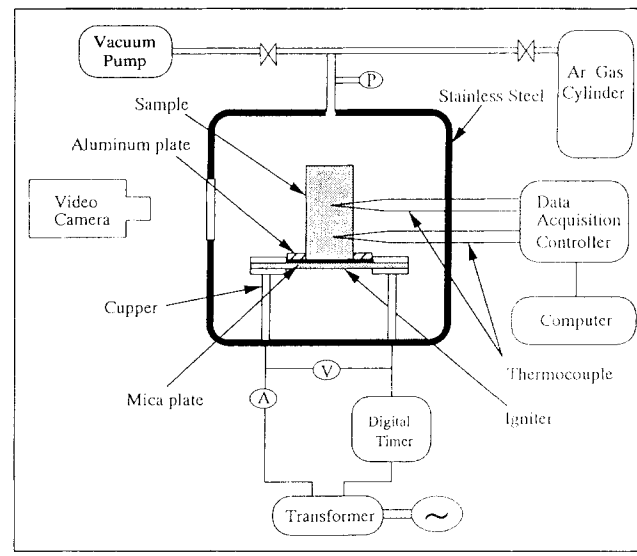


**Figure 1. Experimental apparatus for combustion synthesis of Mg-Ni compressed materials.**

Current address of T. Akiyama: Dept. of Mechanical Engineering, Miyagi National College of Technology, Natori, Japan 981-1239.

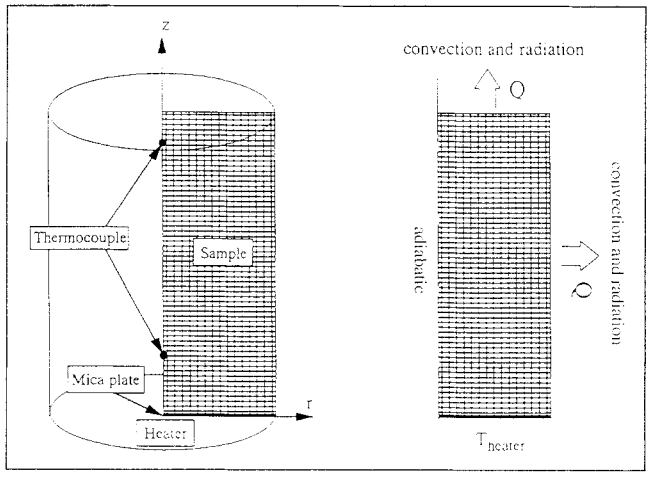


**Figure 2. Grid arrangement for numerical computation with location of thermocouple inserted (60× 15).**

area (10 mm $\phi$) was covered by an alumina plate (2 mm thickness) in order to prevent thermal radiation from the heater to the sample side surface. During the experiment, a bottom end of the sample was kept at a desired constant temperature for 600 s at argon atmosphere. According to a preliminary test, keeping the heater constant temperature was needed for the combustion synthesis of this system, due to weak exothermic heat.

## Numerical Analysis

Fundamental equations of heat transfer are derived in a 2-D cylindrical coordinate, as listed in Table 1; the third term on the righthand side consists of exothermic combustion heat and endothermic heat due to melting of a eutectoid phase of the Mg-Ni system. Thus, this equation is generally available for the combustion synthesis with phase change. Equations 7 to 10 are boundary conditions, meaning that the heat loss from the surface of the sample is due to thermal radiation and natural convection, there is no heat flux (adiabatic) on the central axis, and the mica plate temperature is the same as the heater. The fundamental Eq. 1 was discretized by using the control volume method (Patankar, 1985) and a repeated numerical analysis computed based on an implicit scheme until convergence.

In the computation, much attention is paid to optimize mesh structure. For this purpose, mesh dependence on temperature field is examined for different mesh structures. The computations are done with the help of underrelaxation scheme around the eutectic temperature in the iterative procedure for avoiding divergence during the iteration.

## Property

Table 2 and Figure 3 summarize all properties and process parameters used for the numerical computation.

### *Specific heat, $C_p$*

Data of specific heat of the sample is measured from differential scanning calorimeter (DSC) base line. In the measurement, a piece of the sample (1 mg) was heated at the rate of 1 K per min at argon atmosphere. It is confirmed that the obtained data have good agreement at lower temperature with recently reviewed data of $Mg_2Ni$ by Feufel and Sommer (1995).

**Table 1. Basic Equations for Mathematical Modeling**

$$\rho c\frac{\partial T}{\partial t}=\frac{1}{r}\frac{\partial}{\partial r}\left(rk_e\frac{\partial T}{\partial r}\right)+\frac{\partial}{\partial z}\left(k_e\frac{\partial T}{\partial z}\right)+\rho\left((-\Delta H_c)\frac{df_c}{dt}+(1-f_{c,T_m})(-\Delta H_m)\frac{df_m}{dt}\right) \quad (1)$$

$$\frac{df_c}{dt}=A\exp\left(-\frac{\Delta E}{RT}\right)(1-f_c)^2 \quad (2)$$

$$\begin{aligned}A&=A_1 && (T<T_m)\\&=A_1+(A_2-A_1)/\Delta T && (T_m\le T\le T_m+\Delta T)\\&=A_2 && (T_m+\Delta T<T)\end{aligned} \quad (3)$$

$$\begin{aligned}f_m&=0 && (T<T_m)\\&=(T-T_m)/\Delta T_m && (T_m\le T\le T_m+\Delta T_m)\\&=1 && (T_m+\Delta T_m<T)\end{aligned} \quad (4)$$

I.C.

$$T=T_0 \quad (\text{at } t=0) \quad (5)$$

$$f_c=f_m=0 \quad (\text{at } t=0) \quad (6)$$

B.C.

$$\frac{\partial T}{\partial r}=0 \quad (\text{at } r=0) \quad (7)$$

$$-k_e\frac{\partial T}{\partial r}=h(T-T_g)+\epsilon\sigma(T^4-T_{\text{wall}}^4) \quad (\text{at } r=R) \quad (8)$$

$$T=T_{\text{heater}} \quad (\text{at } z=0) \quad (9)$$

$$-k_e\frac{\partial T}{\partial z}=h(T-T_g)+\epsilon\sigma(T^4-T_{\text{wall}}^4) \quad (\text{at } z=Z) \quad (10)$$

### *Thermal diffusivity, $\alpha$*

A laser flash method (Akiyama et al., 1995b) was employed for the measurement of thermal diffusivity. The procedure of the method is that a pulsed Ruby laser beam flashes the top

**Table 2. Properties Used for Numerical Computation**

| Property | Value | Method/Reference |
|---|---|---|
| *Sample* | | |
| $C_p$ | $483.8+0.6466T$ | DSC |
| $\alpha$ | $2.85\times10^{-5}(1-f_c)+1.39\times10^{-5}f_c$ | Laser Flash method |
| $\rho$ | $2970(1-f_c)+2860f_c$ | Archimedes method |
| $k_e$ | $\alpha\cdot\rho\cdot C_p$ | |
| $\Delta H_c$ | $-372.4\times10^3$ | Feufel and Sommer (1995) |
| $\Delta H_m$ | $158.7\times10^3$ | DSC |
| $A_1$ | $5.46\times10^8$ | DSC |
| $A_2$ | $2.79\times10^9$ | DSC |
| $\Delta E$ | $159\times10^3$ | DSC |
| $\epsilon$ | $0.1(1-f_c)+0.9f_c$ | Aleksander (1996) |
| $h$ | 2.8 (Side), 3.6 (Top) | McAdams method |
| *Mica plate* | | |
| $C_{p,\text{mica}}$ | 837 | Nishikawa and Fujita (1985) |
| $\rho_{\text{mica}}$ | 2600 | Nishikawa and Fujita (1985) |
| $k_{\text{mica}}$ | $4.8\times10^{-4}T+0.371$ | Astronomical Observatory (1991) |

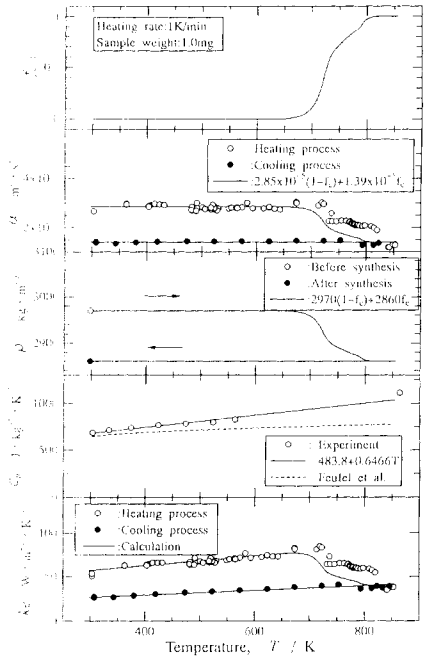


**Figure 3. Temperature dependences of reaction degree, thermal diffusivity, density, specific heat, and thermal conductivity of the sample.**

surface of a disk shaped sample, 10 mm in diameter and 1 mm in thickness at vacuum and then a radiation pyrometer monitors temperature response at the back surface of the sample. From the obtained temperature curve, we can assess thermal diffusivity. The data measured under a heating condition before the reaction gradually decreased with the reaction, and decreased to approximately half under a cooling condition. Significantly, the obtained data was well correlated by weighing equation with reaction degree, as given in Table 2 and Figure 3.

### *Apparent density*

Apparent density of the sample before and after the reaction at room temperature was evaluated based on Archimedes method. With quite a small thermal expansion of metallic magnesium and nickel below 1,000 K, apparent density is regarded as constant before and after the reaction. During the reaction, it varies with reaction degree linearly.

### *Thermal conductivity, $k_e$*

Thermal conductivity of the sample can be evaluated by multiplying the three properties of specific heat, effective thermal diffusivity and apparent density (Akiyama et al., 1997b).

### *Emissivity, $\epsilon$*

According to a previous study (Akiyama et al., 1995a), the sample transforms from the smooth surface with metallic luster to dark, rough skin. Data of nickel with polished-surface and nickel chrome alloy with oxidized surface are employed.

### *Heat-transfer coefficient, h*

McAdams' equation (McAdams, 1954) gives a heat-transfer coefficient ($W \cdot m^{-2} \cdot k^{-1}$) for natural convection in the form of a Nusselt number correlation at a given sample temperature.

### *Reaction rate equation*

Equations 2 and 3 in Table 1 are determined in a previous study as reaction rate equation for the $Mg_2Ni$ combustion synthesis (Akiyama et al., 1997c).

### *Heat of fusion, $\Delta H_m$*

It is known that the Mg-Ni combustion synthesis causes partial melting over a eutectic temperature (Akiyama et al., 1995a). The DSC analysis, done at argon atmosphere using a 1 mg sample, showed that the amount of melting changes significantly with heating rate. Simply speaking, the larger heating rate brings the more melting and vice versa; thus, the melting amount should be correlated by an unreacted degree at 779 K, $1 - f_{c,779\,K}$. For evaluating the intrinsic value of fusion heat $\Delta H_m$ by the extrapolation technique, the data, measured by the DSC analysis, are plotted against the reciprocal of heating rate in Figure 4. The obtained value as $\Delta H_m$ was 158.7 kJ/kg. As a result, effective heat of fusion is expressed by multiplying this value and unreacted degree at 779 K. In addition, the DSC analysis showed that the melting temperature region is from $T_m$ (779 K) to $T_m + \Delta T_m$ (ca. 30 K). From this fact, we can express a rate of melting by Eq. 4 given in Table 1.

## Results and Discussion

### *Mesh dependence*

Using the model developed, we examined mesh dependence upon the computed solution. For this purpose, six different mesh structures with uniform width were prepared, as given in Table 3. The computation conditions were set to be identical as experimental ones. To evaluate quantitatively the mesh dependence on the computed results, we selected three

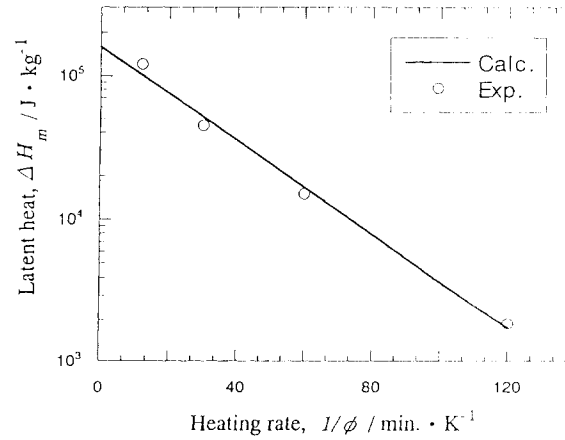


**Figure 4. Apparent latent heat of the sample against heating rate for estimation of true latent heat by an extrapolation technique.**

**Table 3. Mesh Dependence Against Calculated Temperature at Reference Points after 300 s**

| Grid | | Temperature, $T$/K | | |
|---|---|---|---|---|
| No. | $r \times z$ | $A$ | $B$ | $C$ |
| 1 | 10×40 | 839.19 | 819.95 | 818.60 |
| 2 | 15×40 | 848.46 | 829.99 | 828.61 |
| 3 | 5×60 | 850.67 | 832.53 | 831.16 |
| 4 | 10×60 | 854.21 | 836.75 | 835.41 |
| 5 | 15×60 | 854.06 | 836.29 | 834.92 |
| 6 | 15×70 | 854.10 | 836.42 | 834.96 |

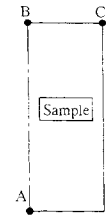


different locations as a reference point. Table 3 gives obtained temperatures at the reference points after just 300 s. Some structures of coarse mesh gave remarkably small values as temperature. For example, between the meshes of No. 1 and No. 6 temperature difference reached as much as 16 K. This implies that the coarse mesh cannot follow actual transient phenomena of heat transfer under this condition. In fact, the maximum difference between Nos. 4 and 5 meshes was 0.059% on the No. 5 mesh basis and between the Nos. 5 and 6 ones (0.016%). From these results, it is judged that the No. 5 mesh structure (15×60) is fine enough for obtaining reasonable solution within error of 0.02%.

### *Comparison to experimental data*

Using the No. 5 mesh structure, the computation was done under experimental conditions. In the experiment of heater temperature of 1,133 K, the temperature was kept to be constant during the experiment. Figure 5 shows calculated results at positions Nos. 1 and 2 in comparison to observed ones. It is found that the observed temperatures of the sample increased gradually, then jumped and finally approached a constant value. The jump is due to an exothermic heat caused by the combustion synthesis. Calculated conversion also simulates this phenomena well.

The observed temperature at the first position (No. 1) showed always slightly higher than at the second one (No. 2) during the experiment, as the calculated temperature showed. As for both the starting time of the temperature jump and its magnitude, there is good agreement between the observed and calculated results. In particular, calculated peak positions simulated observed ones completely, although slight over-evaluation of temperature is found at an initial stage.

### *Influence of melting*

While developing the model, we examined melting effect numerically. To our knowledge, endothermic heat of the melting has been usually neglected in fundamental equations of the combustion synthesis; this is because exothermic heat of combustion is often much too large in comparison to that. According to Kuwabara et al. (1995), so far, only a few models have been devoted to phase-change problems in the combustion synthesis process. However, we should recognize that exothermic heat of combustion synthesis of some intermetallic compounds, including $Mg_2Ni$ synthesis, is relatively small.

The effect of melting was studied by solving two different fundamental equations with and without a term of melting heat. Figure 6 shows temperature curves calculated with and

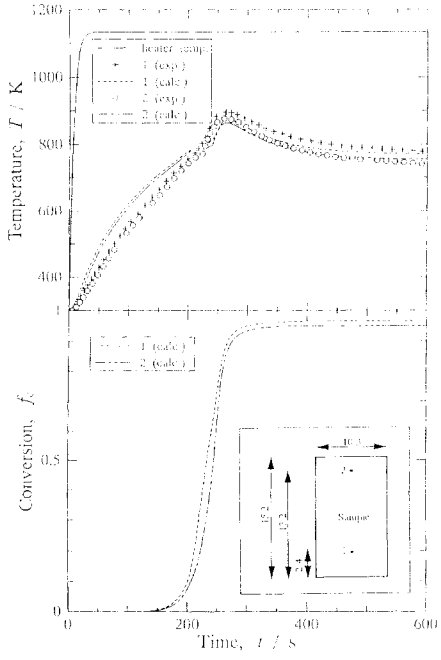


**Figure 5. Observed calculated temperatures during combustion synthesis, together with calculated profiles of conversion ratio (heater temperature: 1,133 K).**

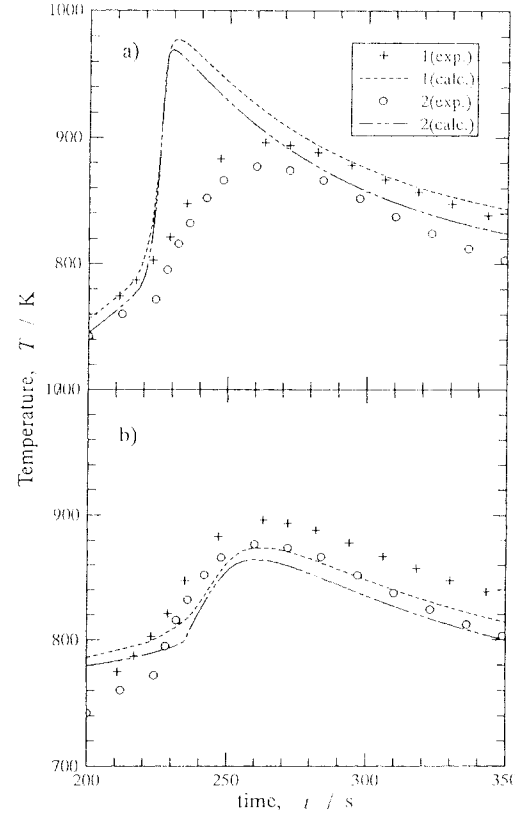


**Figure 6. Influence of latent heat of the sample melting on temperature profiles.**

(a) Without latent heat, (b) with latent heat.

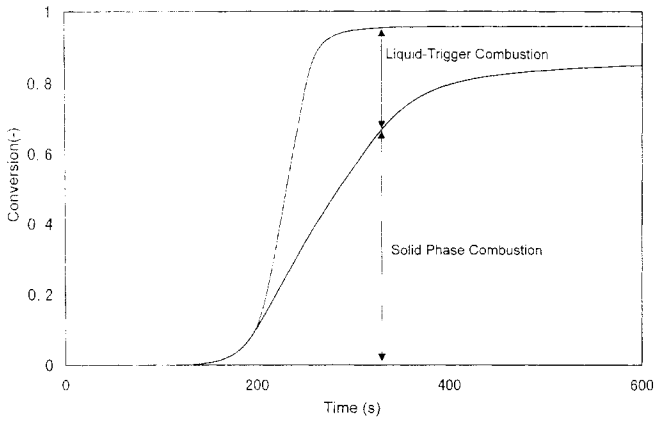


**Figure 7. Comparison between liquid-trigger combustion and solid-phase combustion in conversion curve at position No. 7.**

without the melting effect. It is obvious that the temperature peaks without the melting effect are too sharp, showing abnormal shape, in comparison to the observed one. In addition, temperature profiles at different positions superimpose partially although experimental data are different.

In contrast, the model with the melting effect simulates the observed data well, in which peak shape becomes smooth. This is the reason why we did not neglect the melting effect in the fundamental equations. Partial melting causes *liquid-trigger combustion*. Figure 7 shows a change in the rate of liquid-trigger combustion and solid phase combustion at position No. 1. In this case, the rate of solid-phase combustion was more. However, it is found that the rate of liquid-trigger combustion is not neglected. In particular, this rate will become predominant with increasing heating rate.

### *Influence of radial distribution*

Figure 8 shows radial distributions of temperature and reaction degree within the sample during the reaction. The radial distributions of temperature become larger with time, which is probably caused by increases in both surface temperature and the sample emissivity. Heat loss from the sample surface induces radial distributions of the reaction degree; this leads the lower degree near the sample surface. These results imply that 2-D analysis at least is needed if heat loss from the sample is not neglected.

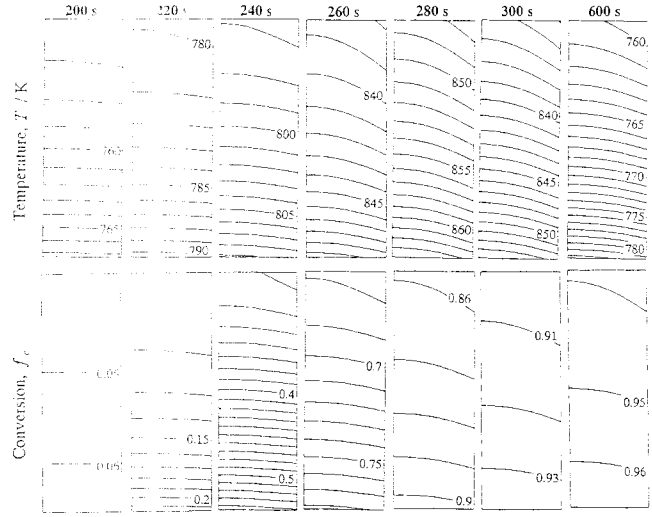


**Figure 8. Distribution changes of temperature and conversion ratio in the sample with time ($\Delta T = 1.0$, $\Delta f = 0.01$.**

## Conclusion

In this study, a total mathematical model has been successfully developed. It simulates transport phenomena in the combustion synthesis process of the Mg-Ni system. The character of the model developed is to take measured properties and reaction rate equation into consideration. In particular, as reaction mechanism, two modes of *solid-phase combustion* and *liquid-trigger combustion* with partial melting are involved.

Comparison between numerical simulation and experimental data showed good agreement. This also offers the benefit of being widely applicable to other systems of the combustion synthesis.

## Acknowledgments

This work was supported by grant-in-aid for scientific research (No. 09450276, No. 50175808) from the Ministry of Education, Science and Culture, Japan.

## Notation

$A$ = frequency factor, $s^{-1}$
$C_p$ = heat capacity, $J \cdot kg^{-1} \cdot K^{-1}$
$\Delta E$ = activation energy, $J \cdot mol^{-1}$
$f$ = conversion
$\Delta H$ = reaction heat, $J \cdot kg^{-1}$
$k$ = thermal conductivity, $W \cdot m^{-1} \cdot K^{-1}$
$r$ = radial coordinate, m
$R$ = universal gas constant, $J \cdot mol^{-1} \cdot K^{-1}$
$t$ = time, s
$z$ = axial coordinate, m

### *Greek letters*

$\alpha$ = thermal diffusivity, $m^2 \cdot s^{-1}$
$\rho$ = density, $kg \cdot m^3$

### *Subscripts*

$c$ = combustion synthesis
$g$ = gas
$m$ = melting
0 = initial
wall = inner wall of stainless steel chamber

## Literature Cited

Advani, A. H., N. N. Thadhani, and H. A. Grebe, "Dynamic Modeling of Self Propagating High Temperature Synthesis of Titanium Carbide Ceramics," *J. Mater. Sci.*, **27**, 3309 (1992).

Akiyama, T., H. Isogai, and J. Yagi, "Combustion Synthesis of Magnesium Nickel," *Int. J. of Self-Propagating High-Temperature Synthesis*, **4**, 69 (1995a).

Akiyama, T., T. Fukutani, R. Takahashi, J. Yagi, H. Ohta, and Y. Waseda, "Microencapsulation of Mg-Ni Hydrogen Storage Alloy," *AIChE J.*, **41**, 1349 (1995b).

Akiyama, T., T. Tazaki, R. Takahashi, and J. Yagi, "Optimization of Microencapsulating and Compacting Conditions for Hydrogen Storage Alloy," *J. of Alloys and Compounds*, **236**, 171 (1996a).

Akiyama, T., T. Fukutani, Reijiro Takahashi, and Jun-ichiro Yagi, "Heat Storage Rate of Magnesium Nickel Hydride," *Mat. Trans. JIM*, **37**, 1014 (1996b).

Akiyama, T., H. Isogai, and J. Yagi, "Hydriding Combustion Synthesis for Production of Hydrogen Storage Alloy," *J. of Alloys and Compounds*, **1**, 252 (1997a).

Akiyama, T., H. Isogai, H. Nogami, R. Takahashi, and J. Yagi, "Thermal Conductivity During Combustion Synthesis for Production of Hydrogen Storage Alloy," *Experimental Heat Transfer, Fluid Mechanics and Thermodynamics*, 2567, 4 (1997b).

Akiyama, T., H. Isogai, and J. Yagi, "Reaction Rate of Combustion Synthesis of Intermetallic Compound," *Powder Technol.*, **178**, 95 (1998c).

Aleksander, Sara, *Physical Sciences Data* 21, *Radiant Properties of Materials*, Elsevier, p. 177 (1986).

Feufel, H., and F. Sommer, "Thermodynamic Investigations of Binary Liquid and Solid Cu-Mg and Mg-Ni Alloys and Ternary Liquid Cu-Mg-Ni Alloys," *J. Alloys Comp.*, 224, 42 (1995).

Kuwabara, M., N. Ohtuka, and S. Asai, "Numerical Analysis of Self-Propagating High-Temperature Synthesis (SHS) Combustion Wave Based on Movable Nonuniform Grid," *Int. J. of Self-Propagating High-Temperature Synthesis*, **4**, 253 (1995).

McAdams, W. H., *Heat Transmission*, 3*rd*, McGraw-Hill, New York (1954).

Nishikawa, K., and Y. Fujita, *Heat Transfer*, Rikogaku Publisher, Tokyo, p. 452 (1985).

National Astronomical Observatory, "Science Chronological Table," *Maruzen*, Tokyo, p. 477 (1991).

Patankar, S. V., *Numerical Heat Transfer and Fluid Flow*, McGraw-Hill, New York (1980).

Puszynski, J., J. Degrev, and V. Hlavacek, "Modeling of Exothermic Solid-Solid Noncatalytic Reactions," *Ind. Eng. Chem. Res.*, **26**, 1424 (1987).

Varma, A., G. Cao, and M. Morbidelli, "Self-Propagating Solid-Solid Noncatalytic Reaction in Finite Pellets," *AIChE J.*, **36**, 1032 (1990).

*Manuscript received Mar. 10, 1997, and revision received Dec. 1, 1997.*